

# Supporting Information: Effects of impurity gases on interfaces of the hydrogen-water-decane three-phase system: A square gradient theory investigation

Yafan Yang<sup>1,\*</sup>, Jingyu Wan<sup>1</sup>, Jingfa Li<sup>2</sup>, Weiwei Zhu<sup>3</sup>, Guangsi Zhao<sup>1</sup>, Xiangyu Shang<sup>1,\*</sup>

<sup>1</sup>State Key Laboratory for Geomechanics and Deep Underground Engineering, China University of Mining and Technology, Xuzhou 221116, P. R. China

<sup>2</sup>School of Mechanical Engineering and Hydrogen Energy Research Center, Beijing Institute of Petrochemical Technology, Beijing 102617, P. R. China

<sup>3</sup>Department of Engineering Mechanics, Tsinghua University, Beijing 100084, P. R. China

\*Corresponding Author: Yafan Yang. Email: yafan.yang@cumt.edu.cn; ORCID: 0000-0001-7119-623X;

Xiangyu Shang. Email: xyshang@cumt.edu.cn; ORCID: 0000-0003-4738-2424

## Appendix A.

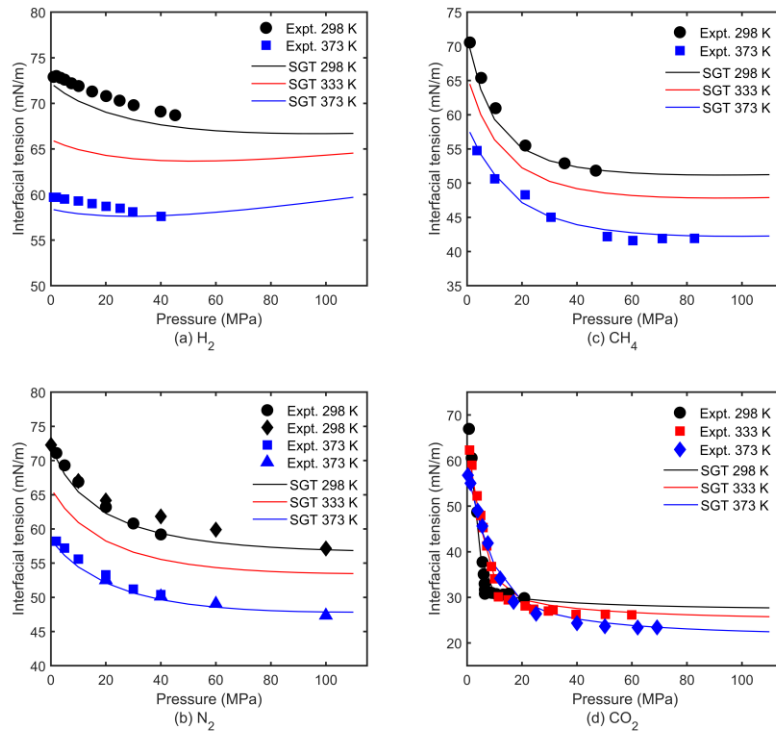


**Fig. A1** Pressure dependence of IFT in the gas-H<sub>2</sub>O 2-phase systems: (a) H<sub>2</sub>, (b) N<sub>2</sub>, (c) CH<sub>4</sub>, and (d) CO<sub>2</sub> at various temperatures. Predictions from SGT are shown as lines and the experimental data from Refs. S1-S7 are

shown as filled symbols.

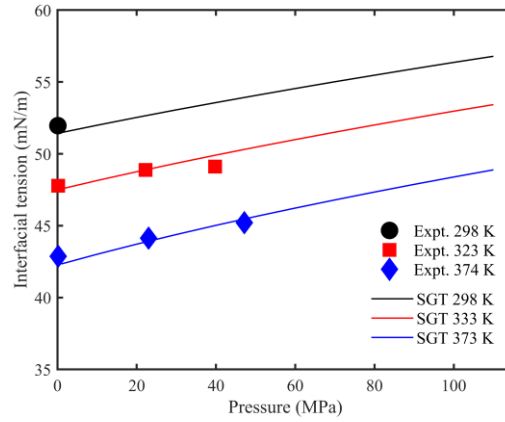


**Fig. A2** Pressure dependence of IFT in the H<sub>2</sub>O-decane 2-phase systems at various temperatures. Predictions from SGT are shown as lines and the experimental data from Ref. S8 are shown as filled symbols.

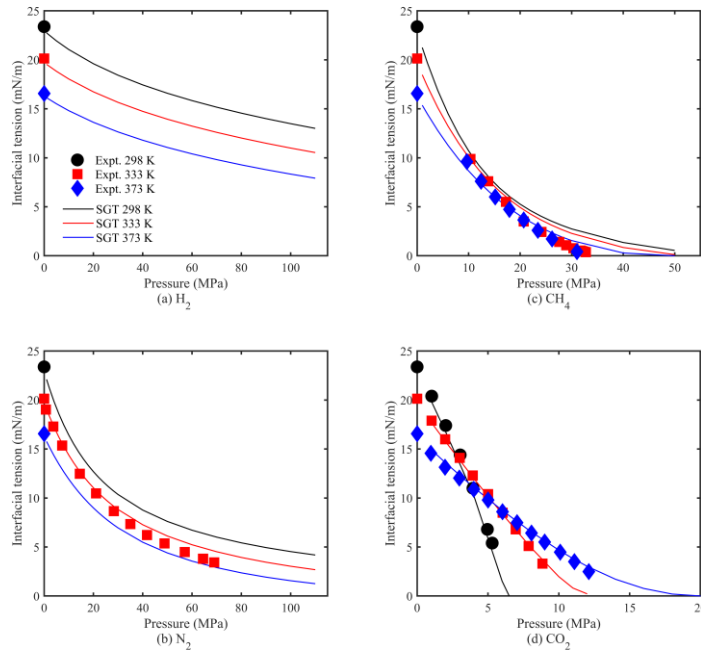


**Fig. A3** Pressure dependence of IFT in the gas-decane 2-phase systems: (a) H<sub>2</sub>, (b) N<sub>2</sub>, (c) CH<sub>4</sub>, and (d) CO<sub>2</sub> at various temperatures. Predictions from SGT are shown as lines and the experimental data from Refs. S9-S14 are shown as filled symbols.

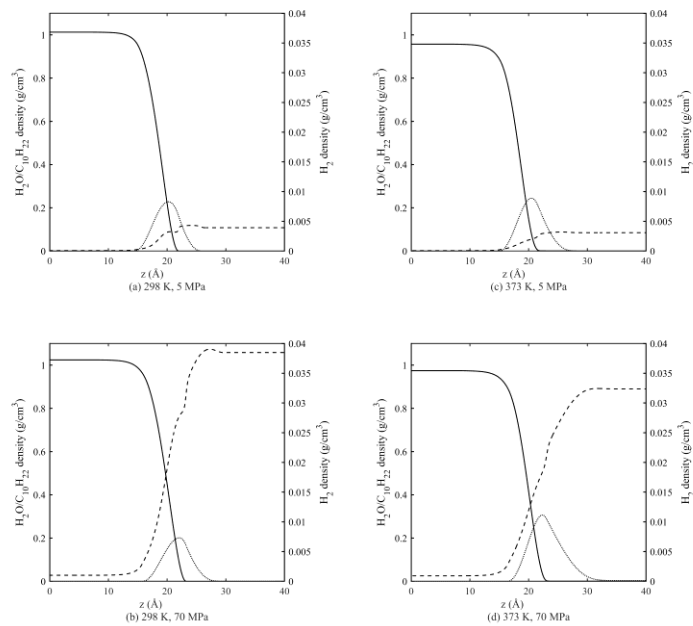


**Fig. A4** Equilibrium distributions of different species in the  $\text{H}_2$ - $\text{H}_2\text{O}$ - $\text{C}_{10}\text{H}_{22}$  3-phase system for the interface between  $\text{H}_2\text{O}$ -rich phase and  $\text{H}_2$ -rich phase at (a) 298 K, 5 MPa, (b) 298 K, 70 MPa, (c) 373 K, 5 MPa, and (d) 373 K, 70 MPa. The solid, dotted, and dashed lines denote  $\text{H}_2\text{O}$ , decane, and  $\text{H}_2$ , respectively. The data are taken from Ref. S15.

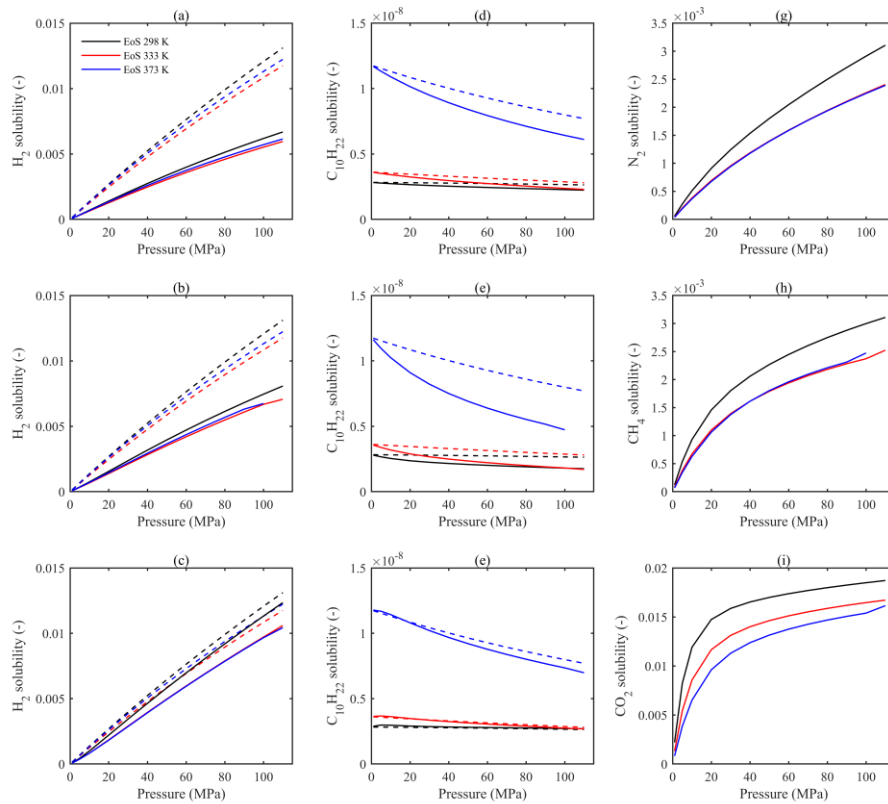


**Fig. A5** Solubilities in the H<sub>2</sub>O-rich phase in gas-H<sub>2</sub>-H<sub>2</sub>O-C<sub>10</sub>H<sub>22</sub> 3-phase systems. Top, middle, and bottom panels show solubilities in systems containing N<sub>2</sub>, CH<sub>4</sub>, and CO<sub>2</sub>, respectively. The data for dashed lines are taken from Ref. S15.

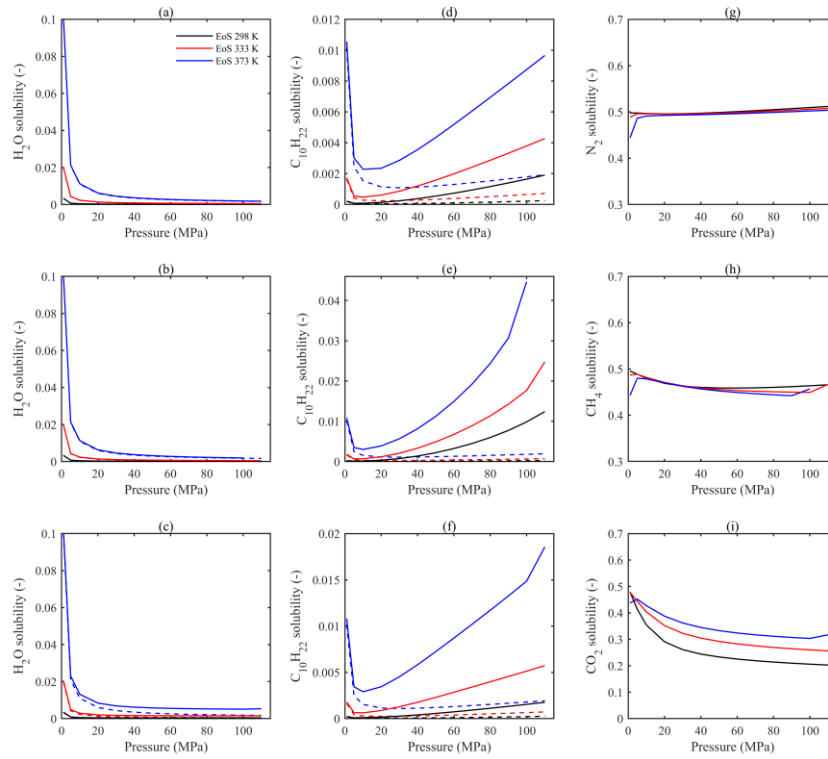


**Fig. A6** Solubilities in the  $H_2$ -rich phase in gas- $H_2$ - $H_2O$ - $C_{10}H_{22}$  3-phase systems. Top, middle, and bottom panels show solubilities in systems containing  $N_2$ ,  $CH_4$ , and  $CO_2$ , respectively. The data for dashed lines are taken from Ref. S15.

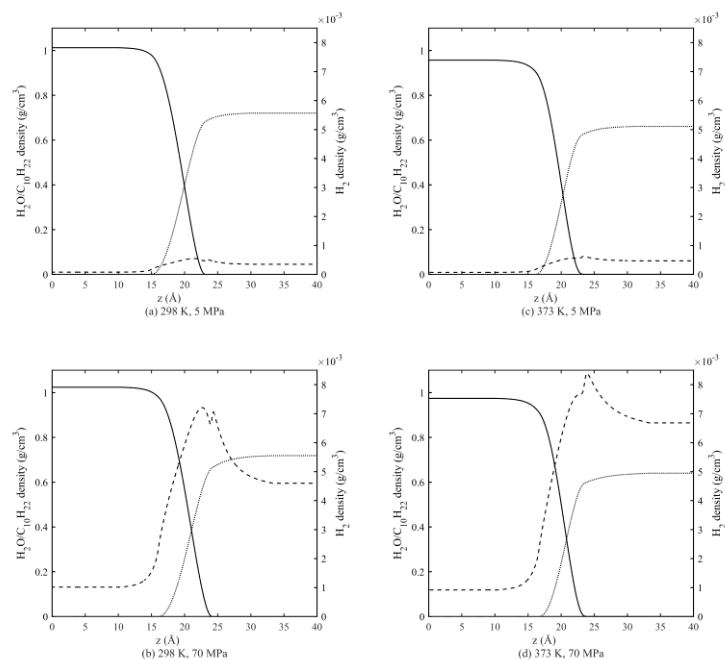


**Fig. A7** Equilibrium distributions of different species in the  $\text{H}_2\text{-H}_2\text{O-C}_{10}\text{H}_{22}$  3-phase system for the interface between  $\text{H}_2\text{O}$ -rich phase and  $\text{C}_{10}\text{H}_{22}$ -rich phase at (a) 298 K, 5 MPa, (b) 298 K, 70 MPa, (c) 373 K, 5 MPa, and (d) 373 K, 70 MPa. The solid, dotted, and dashed lines denote  $\text{H}_2\text{O}$ , decane, and  $\text{H}_2$ , respectively. The data are taken from Ref. S15.

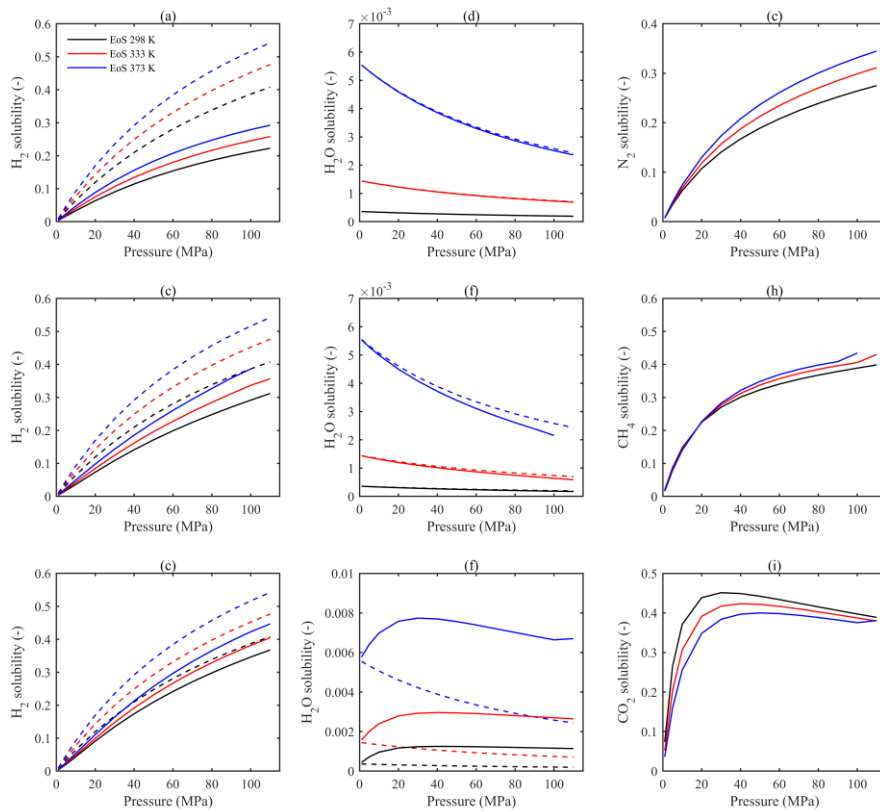


**Fig. A8** Solubilities in the  $C_{10}H_{22}$ -rich phase in gas- $H_2$ - $H_2O$ - $C_{10}H_{22}$  3-phase systems. Top, middle, and bottom panels show solubilities in systems containing  $N_2$ ,  $CH_4$ , and  $CO_2$ , respectively. The data for dashed lines are taken from Ref. S15.

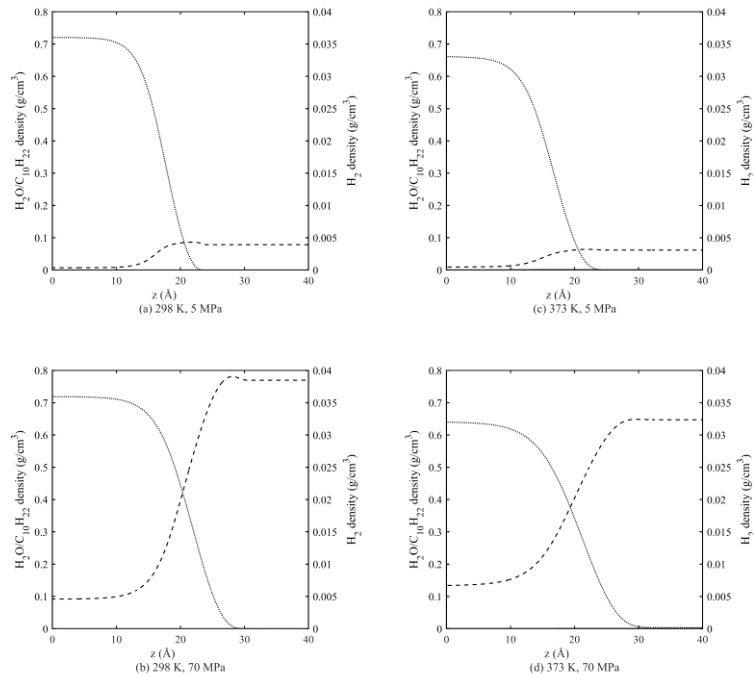


**Fig. A9** Equilibrium distributions of different species in the  $\text{H}_2$ - $\text{H}_2\text{O}$ - $\text{C}_{10}\text{H}_{22}$  3-phase system for the interface between  $\text{H}_2$ -rich phase and  $\text{C}_{10}\text{H}_{22}$ -rich phase at (a) 298 K, 5 MPa, (b) 298 K, 70 MPa, (c) 373 K, 5 MPa, and (d) 373 K, 70 MPa. The solid, dotted, and dashed lines denote  $\text{H}_2\text{O}$ , decane, and  $\text{H}_2$ , respectively. The data are taken from Ref. S15.

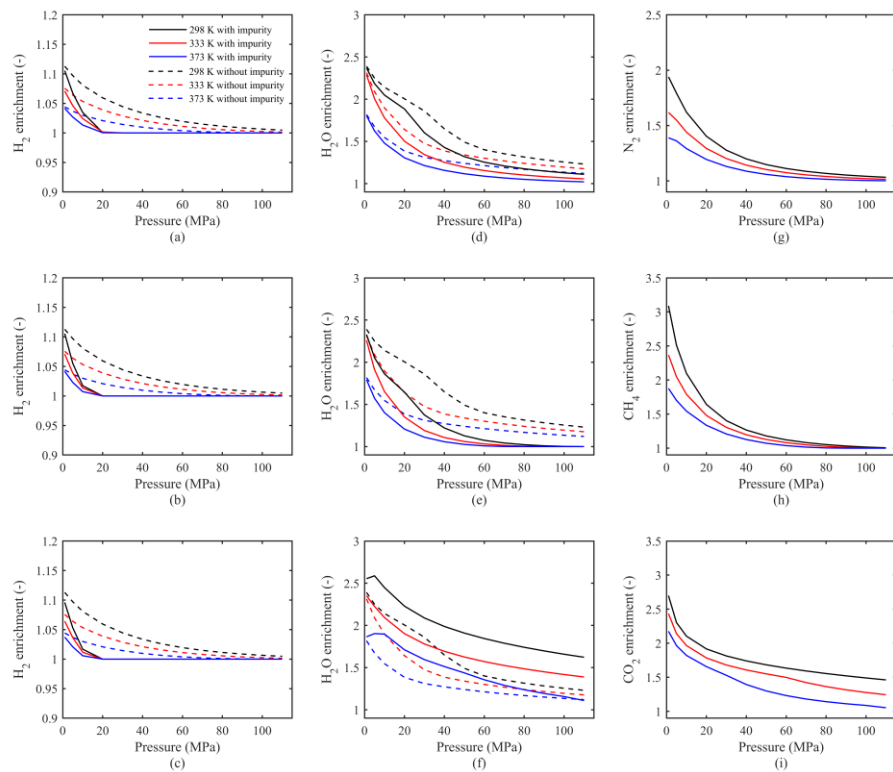


**Fig. A10** Component enrichments of the H<sub>2</sub>-H<sub>2</sub>O-C<sub>10</sub>H<sub>22</sub> interface. Top, middle, and bottom panels show surface excesses in systems containing N<sub>2</sub>, CH<sub>4</sub>, and CO<sub>2</sub>, respectively. Dashed lines are taken from Ref. S15.

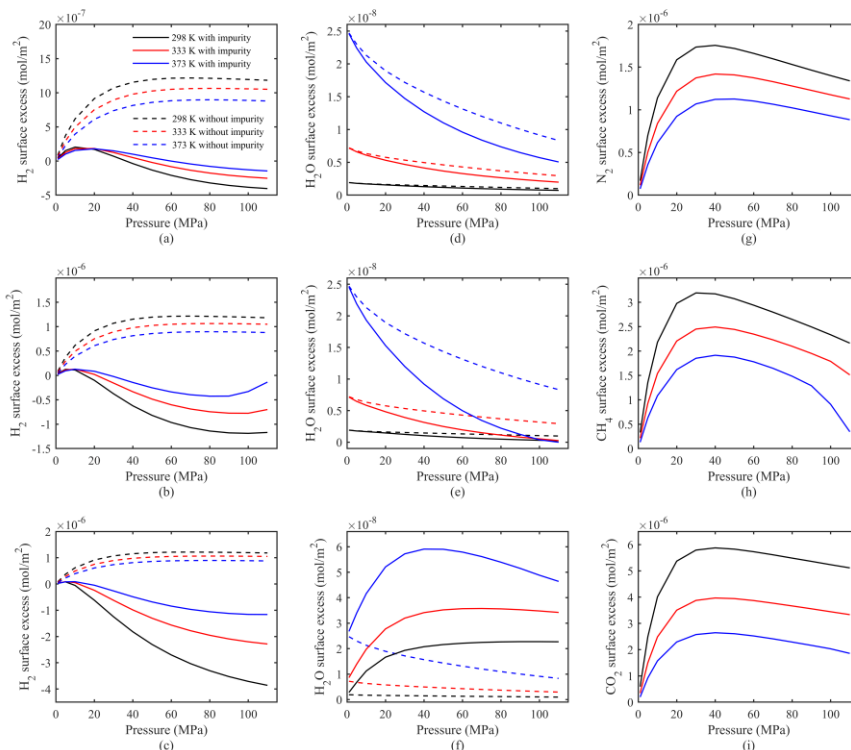


**Fig. A11** Component surface excesses of the  $\text{H}_2\text{-H}_2\text{O-C}_{10}\text{H}_{22}$  interface. Top, middle, and bottom panels show surface excesses in systems containing  $\text{N}_2$ ,  $\text{CH}_4$ , and  $\text{CO}_2$ , respectively. Dashed lines are taken from Ref. S15.

## References

- S1. Chow, Y. F., Maitland, G. C., & Trusler, J. M. (2018). Interfacial tensions of  $(\text{H}_2\text{O}+\text{H}_2)$  and  $(\text{H}_2\text{O}+\text{CO}_2+\text{H}_2)$  systems at temperatures of (298–448) K and pressures up to 45 MPa. *Fluid Phase Equilibria*, 475, 37–44.
- S2. Chow, Y. F., Maitland, G. C., & Trusler, J. M. (2020). Erratum to “Interfacial tensions of  $(\text{H}_2\text{O}+\text{H}_2)$  and  $(\text{H}_2\text{O}+\text{CO}_2+\text{H}_2)$  systems at temperatures of (298 to 448) K and pressures up to 45 MPa” [*Fluid Phase Equil.* 475 (2018) 37–44].
- S3. Chow, Y. F., Maitland, G. C., & Trusler, J. M. (2016). Interfacial tensions of the  $(\text{CO}_2+\text{N}_2+\text{H}_2\text{O})$  system at temperatures of (298 to 448) K and pressures up to 40 MPa. *The Journal of Chemical Thermodynamics*, 93, 392–403.
- S4. Wiegand, G., & Franck, E. U. (1994). Interfacial tension between water and non-polar fluids up to 473 K and 2800 bar. *Berichte der Bunsengesellschaft für physikalische Chemie*, 98(6), 809–817.
- S5. Kashefi, K., Pereira, L. M., Chapoy, A., Burgass, R., & Tohidi, B. (2016). Measurement and modelling of interfacial tension in methane/water and methane/brine systems at reservoir conditions. *Fluid Phase Equilibria*, 409, 301–311.
- S6. Sachs, W., & Meyn, V. (1995). Pressure and temperature dependence of the surface tension in the system natural gas/water principles of investigation and the first precise experimental data for pure methane/water

---

at 25 C up to 46.8 MPa. *Colloids and Surfaces A: Physicochemical and Engineering Aspects*, 94(2-3), 291-301.

S7. Pereira, L. M., Chapoy, A., Burgass, R., Oliveira, M. B., Coutinho, J. A., & Tohidi, B. (2016). Study of the impact of high temperatures and pressures on the equilibrium densities and interfacial tension of the carbon dioxide/water system. *The Journal of Chemical Thermodynamics*, 93, 404-415.

S8. Georgiadis, A., Maitland, G., Trusler, J. M., & Bismarck, A. (2011). Interfacial tension measurements of the (H<sub>2</sub>O+n-decane+CO<sub>2</sub>) ternary system at elevated pressures and temperatures. *Journal of Chemical & Engineering Data*, 56(12), 4900-4908.

S9. Linstrom, P. J., & Mallard, W. G. (2001). The NIST Chemistry WebBook: A chemical data resource on the internet. *Journal of Chemical & Engineering Data*, 46(5), 1059-1063.

S10. Pereira, L. M., Chapoy, A., Burgass, R., & Tohidi, B. (2016). Measurement and modelling of high pressure density and interfacial tension of (gas+n-alkane) binary mixtures. *The Journal of Chemical Thermodynamics*, 97, 55-69.

S11. Stegemeier, G. L., Pennington, B. F., Brauer, E. B., & Hough, E. W. (1962). Interfacial tension of the methane-normal decane system. *Society of Petroleum Engineers Journal*, 2(03), 257-260.

S12. Amin, R., & Smith, T. N. (1998). Interfacial tension and spreading coefficient under reservoir conditions. *Fluid phase equilibria*, 142(1-2), 231-241.

S13. Pan, Z., & Trusler, J. M. (2023). Measurement and modelling of the interfacial tensions of CO<sub>2</sub>+decane-iododecane mixtures at high pressures and temperatures. *Fluid Phase Equilibria*, 566, 113700.

S14. Georgiadis, A., Llovel, F., Bismarck, A., Blas, F. J., Galindo, A., Maitland, G. C., Trusler, J. M. & Jackson, G. (2010). Interfacial tension measurements and modelling of (carbon dioxide+n-alkane) and (carbon dioxide+ water) binary mixtures at elevated pressures and temperatures. *The Journal of Supercritical Fluids*, 55(2), 743-754.

S15. Yang, Y., Wan, J., Li, J., Zhao, G., & Shang, X.. (2023). Molecular modeling of interfacial properties of the hydrogen+water+decane mixture in three-phase equilibrium. arXiv preprint, arXiv: 2307.15356.